Microtubule-targeting agents inhibit angiogenesis at subtoxic concentrations, a process associated with inhibition of Rac1 and Cdc42 activity and changes in the endothelial cytoskeleton

Marcel N.A. Bijman,[1] Geerten P. van Nieuw Amerongen,[2] Nancy Laurens,[2] Victor W.M. van Hinsbergh,[1,2] and Epie Boven[1]

[1]Departments of Medical Oncology and [2]Physiology, Vrije Universiteit Medical Center, Amsterdam, the Netherlands

Abstract

Conventional anticancer agents may display antiangiogenic effects, but the underlying mechanism is poorly understood. We determined the antiangiogenic properties of cisplatin, doxorubicin, and the microtubule-targeting agents docetaxel, epothilone B, and vinblastine at concentrations not affecting cell proliferation. We also assessed tubulin and actin morphology and the activity of two key molecules in cell motility, the small Rho GTPases Cdc42 and Rac1. The highest non-toxic concentration (HNTC) of each drug was defined as the concentration inhibiting a maximum of 10% human umbilical vein endothelial cell growth on a 1-hour drug exposure, being for cisplatin 10 μmol/L, doxorubicin 100 nmol/L, docetaxel 10 nmol/L, epothilone B 1 nmol/L, and vinblastine 10 nmol/L. Comparative endothelial cell functional assays using HNTCs for an exposure time of 1 hour indicated that endothelial cell migration in the wound assay, endothelial cell invasion in a transwell invasion system, and endothelial cell formation into tubelike structures on a layer of Matrigel were significantly inhibited by docetaxel, epothilone B, and vinblastine ($P < 0.05$), but not by cisplatin and doxorubicin. Docetaxel was slightly more efficient in the inhibition of endothelial cell motility than epothilone B and vinblastine. Fluorescence microscopy revealed that only the microtubule-targeting agents affected the integrity of the tubulin and F-actin cytoskeleton, which showed disturbed microtubule structures, less F-actin stress fiber formation, and appearance of nuclear F-actin rings. These observations were associated with early inhibition of Rac1 and Cdc42 activity. In conclusion, HNTCs of microtubule-targeting agents efficiently reduce endothelial cell motility by interference with microtubule dynamics preventing the activation of Rac1/Cdc42 and disorganizing the actin cytoskeleton. [Mol Cancer Ther 2006;5(9):2348–57]

Introduction

Recent interest has focused on the potential antiangiogenic properties of cytotoxic agents that specifically target the cell motility apparatus by affecting the dynamics of microtubules, among which are the taxanes, epothilones, and Vinca alkaloids (1). Taxanes, such as paclitaxel and docetaxel, induce stability of microtubules, whereby the dynamic reorganization and depolymerization are inhibited. Taxanes can inhibit endothelial cell motility and proliferation, which leads to disrupted vessel formation on Matrigel or the chick chorioallantoic membrane, decreased vessel sprouting from aortic rings embedded in Matrigel, and reduction of newly formed blood vessels in tumor-bearing mice (2–6). Epothilones are structurally unrelated to taxanes but share their ability to stabilize microtubules (7). Evidence for antiangiogenic properties of epothilone B has been provided by the observation that vessel formation was inhibited *in vitro* (8) and by studies on frequent low-dose administration, which resulted in inhibition of proliferation of endothelial cells in culture (9). Vinca alkaloids show a different mode of action than taxanes and epothilones: they inhibit both tubulin polymerization and mitotic spindle formation. *In vitro* endothelial cell proliferation, motility, and organization, together with blood vessel formation in tumors *in vivo*, were found to be potently inhibited by vinblastine (10, 11).

Whereas antiangiogenic properties of microtubule-targeting agents have been recognized, it is also established that drug concentrations lower than those inhibiting endothelial cell proliferation are able to suppress microtubule dynamics (1). Interference with microtubule dynamics will affect not only endothelial cell motility but also other cellular processes. For instance, the activity of Rho GTPases, a family of molecules that tightly coordinate motility, might be disturbed. Rho GTPases are activated on binding of tumor-secreted vascular endothelial growth factor to specific receptors on the surface of endothelial cells (12, 13). One of the best known family members, Cdc42, regulates polarity of the cell,

Received 5/2/06; revised 6/13/06; accepted 7/11/06.

Grant support: Sanofi-Aventis (M.N.A. Bijman) and the Netherlands Heart Foundation grant T2003-0032 (G.P. van Nieuw Amerongen).

The costs of publication of this article were defrayed in part by the payment of page charges. This article must therefore be hereby marked advertisement in accordance with 18 U.S.C. Section 1734 solely to indicate this fact.

Correspondence: Epie Boven, Department of Medical Oncology, Vrije Universiteit Medical Center, De Boelelaan 1117, 1081 HV Amsterdam, the Netherlands. Phone: 31-20-444-4336; Fax: 31-20-444-4079. E-mail: e.boven@vumc.nl

doi:10.1158/1535-7163.MCT-06-0242

enabling motility to be initiated in the desired direction (14). Moreover, the orientation of the centrosome, the main microtubule-organizing center of the cell, towards the leading edge of the cell depends on Cdc42 function (15). Another prominent Rho GTPase family member, Rac1, induces the formation of extensions (lamellipodia) and stimulates actin polymerization at the leading edge of the cell, together with the formation of new adhesion sites to the matrix (16). Member RhoA mediates assembly and contraction of actin-myosin filaments in the cell body and at the rear, which will result in a forward motion (17).

Microtubules operate in close collaboration with the dynamics of the actin cytoskeleton and together they orchestrate cell motility (18). One of the hallmarks of migrating cells is the formation of contractile actin bundles through the cell body in the direction of movement. These actin cables (stress fibers) form focal adhesions at the site of the cell membrane and are linked with myosin filaments that are able to contract and, thus, stimulate motility (16). Because of actin polymerization in the leading edge of the cell, a retrograde flow of actin is formed, which leads to buckling and breakage of actin-associated microtubules. These broken microtubules, in turn, polymerize in the direction of movement, thereby activating Rac1 (18). It is likely that this positive feedback loop and the interactions with actin are prone to become disturbed after microtubule dysfunction.

Research on mechanistic changes underlying the inhibition of endothelial cell motility by microtubule-targeting agents is limited. Most studies on antiangiogenic effects by these compounds focused on inhibition of motility and reduction of vessel formation. In the experiments, often employed were toxic drug concentrations that also inhibit endothelial cell proliferation. Therefore, we designed a study in which the antiangiogenic properties of classic cytotoxic agents affecting microtubules, docetaxel, epothilone B, and vinblastine, were examined with the use of subtoxic as well as equitoxic concentrations and we included two other standard anticancer agents, cisplatin and doxorubicin, which both affect DNA integrity. We also examined the effects of microtubule dynamics disruption on the integrity of the actin cytoskeleton. In addition, activities of Rac1 and Cdc42 were measured to obtain insight into a possible interference in the regulation of endothelial cell motility on the level of Rho GTPases by the anticancer agents.

Materials and Methods

Cell Culture

Human umbilical vein endothelial cells (HUVEC) were isolated from fresh umbilical cords according to the procedure described by Van Hinsbergh and Draijer (19). HUVECs were cultured in gelatin-coated tissue culture flasks in complete medium, M199 medium (Invitrogen, Breda, the Netherlands) containing 10% human serum (Invitrogen), 10% FCS (Invitrogen), 300 mg/mL L-glutamine, 100 units/mL penicillin, 100 μg/mL streptomycin (BioWhittaker, Verviers, Belgium), 5 IU/mL heparin, and 50 μg/mL endothelial cell growth factor (isolated from bovine brain; ref. 20) at 37°C in 5% CO_2. HUVECs were used in passages 2 to 4.

In vitro Antiproliferative Assay

The antiproliferative effects of cisplatin (Bristol-Myers Squibb, Woerden, the Netherlands), doxorubicin (Pharmachemie, Haarlem, the Netherlands), docetaxel (Sanofi-Aventis, Antony, France), epothilone B (Novartis, Basel, Switzerland), and vinblastine (Eli-Lilly, Houten, the Netherlands) were analyzed with the 3-(4,5-dimethylthiazol-2-yl)-2,5-diphenyltetrazolium bromide (MTT) assay. Cells were plated in quadruplicate in culture medium in 96-well plates at 3,000 per well and were exposed to a drug concentration range for 1 hour. After washing, cells were grown in culture medium for an additional 96-hour period. The number of viable cells was determined by addition of MTT (Sigma Aldrich, Zwijndrecht, the Netherlands). The extinction of the formazan product was measured at 540 nm on a Multiscan plate reader (Thermo Biosciences, Breda, the Netherlands). Results were expressed in IC_{50} and IC_{10} values, being the drug concentrations responsible for 50% and 10% cell growth inhibition, respectively, as compared with control cell growth. The IC_{10} concentration, the highest non-toxic concentration (HNTC) of a drug, was used in all further experiments and was checked in parallel MTT assays for each experiment.

Migration Assay

HUVECs were seeded in duplicate in gelatin-coated wells of a 24-well plate and grown to confluence. Cells were or were not treated with drugs (HNTC) for 1 hour in culture medium. A scratch wound was applied in two perpendicular directions in the confluent cell-layer with a sterile pipette tip. Immediately after wounding (0 hours) and at time points 4, 8, and 12 hours, wounds were captured at ×25 magnification with a confocal laserscan microscope (TCS 4D; Leica, Jena, Germany) and Q500MC software (Leica). At all indicated time points, the wound width was measured in four areas and compared with the initial width at 0-hour time point (set at 100%).

Invasion Assay

Endothelial cell invasion was measured in a 24-well plate transwell system (Falcon, Woerden, the Netherlands) containing inserts with a fluorescence-blocking filter of 8 μm pore size (HTS fluoroblock; Falcon). The inserts were coated on the bottom with 2 μg/mL fibronectin (ICN, Zoetermeer, the Netherlands), washed with PBS (BioWhittaker), and coated on the upper side with 5 μg of extracellular matrix gel (Sigma-Aldrich) in 100 μL of PBS. HUVECs (2×10^5) were seeded on top of the extracellular matrix gel layer (duplicate experimental samples) and allowed to settle for 4 hours. Then, HUVECs were exposed to drugs (HNTC) for 1 hour or were left untreated (control) in culture medium followed by replacement of drug-containing medium by fresh culture medium in the upper compartment. Culture medium, enriched with 25 ng/mL recombinant human vascular endothelial growth factor (Biosource, Nivelles, Belgium) as a chemoattractant, was

added to the lower compartment. The cells were allowed to invade for 24 hours. Thirty minutes before analysis, 5 μmol/L calcein-AM (Molecular Probes, Leiden, the Netherlands) was added to the lower compartment, a substance that can be intracellularly converted to the polar fluorochrome calcein. Calcein fluorescence in the lower compartment was measured in a spectrafluor multiplate reader (Tecan, Gorinchem, the Netherlands) at λ_{ex} 492 nm and λ_{em} 535 nm.

Organization Assay

Wells of a 24-well plate were coated with 1 mg/100 μL extracellular matrix gel. HUVECs were pretreated or not with drugs (HNTC) for 1 hour in M199/0.1% bovine serum albumin (ICN) and 10^5 cells were seeded in 1 mL of fresh M199/0.1% bovine serum albumin on top of the extracellular matrix gel. After 24 hours, HUVEC organization patterns were captured by confocal laserscan microscopy and a video camera attached to a computer with Q500MC software (Leica) at ×25 magnification. The number of HUVEC interconnections was calculated in the obtained images and expressed as a percentage of the number of connections formed by untreated cells (set at 100%).

Immunocytochemistry

HUVECs were seeded and grown to confluence on glass coverslips coated with 1% gelatin cross-linked with 0.5% glutaraldehyde in a 24-well plate. Cells were then treated or not with drugs (HNTC) for 1 hour. By gently stripping a layer of cells off the matrix with a 1-mm-thick polyvinylidene difluoride membrane strip (Millipore, Etten-Leur, the Netherlands), a wound was formed in the confluent cell layer. Cells were washed twice with medium and culture medium was added for an 8-hour period, after which cells were fixed with 3.7% formaldehyde without prior PBS washing steps to preserve cytoskeletal integrity. Fixed cells were made permeable with 0.2% Triton X-100 (Sigma-Aldrich) in PBS and incubated with a monoclonal antibody against β-tubulin (1:50; Molecular Probes) for 2 hours in 3% bovine serum albumin/PBS. After washing, cells were incubated with Hoechst 33342 (1:500; Sigma-Aldrich) for nuclear staining and rhodamine-conjugated phalloidin (1:200; Molecular Probes) for F-actin staining. A secondary FITC-labeled mouse-immunoglobulin G targeting antibody (1:120; DAKO, Amsterdam, the Netherlands) was used to visualize β-tubulin. After three washing steps of 15 minutes, coverslips were mounted in Vecta Shield (Vector Laboratories, Burlingame, CA) and digital imaging microscopic analysis was done on a Zeiss Axiovert 200 Marianas inverted microscope (Zeiss, Leusden, the Netherlands). Images were captured by a digital camera (Sensicam, Cooke, Tonawanda, NY), applying identical exposure periods, through a 10× or 40× air lens and analyzed and processed with Slidebook software (version 4.0; Intelligent Imaging Innovations, Denver, CO). The relative intensity of tubulin staining was obtained by calculation of the mean intensity signal above an arbitrary threshold.

Rac1/Cdc42 Activity Assay

HUVECs were grown to 80% confluence on gelatin-coated 10-cm Petri dishes and rendered quiescent in M199 containing 1% human serum and 1% FCS overnight. Rac1/Cdc42 activation was provoked by addition of complete culture medium, whereas at the same time drugs (HNTC) were added or not. After 1 hour, Rac1/Cdc42 activity was analyzed with the Rac/Cdc42 Activation Assay Kit (Chemicon, Chandlers Ford, United Kingdom) according to instructions provided by the manufacturer. In brief, after washing, cells were lysed in assay buffer (supplemented with 0.5 mmol/L trypsin inhibitor, 0.5 μg/mL leupeptin, and 1 mmol/L phenylmethylsulfonyl fluoride) and centrifuged to remove cell debris. To determine total Rac1/Cdc42 levels, 40 μL of each sample were stored at −80°C for separate analysis. The remaining 960 μL of the supernatant were incubated with 10 μg of agarose-conjugated p21-binding domain of p21-activated protein kinase-1, which binds both activated Rac1 and Cdc42, for 1 hour at 4°C with tumbling. Agarose beads with bound active Rac1/Cdc42 were washed four times in assay buffer, resuspended in 30 μL of SDS sample buffer, and boiled for 10 minutes.

Active (GTP-bound) and total Rac1/Cdc42 protein levels in each sample were analyzed by Western blot. Samples obtained from the Rac1/Cdc42 activity assay were subjected to 12% PAGE (130 V, 2 hours). The separated proteins were transferred to a polyvinylidene difluoride membrane (Millipore) by electrotransfer (400 mA, 2 hours). The blots were blocked with 10% milk (Protifar; Nutricia, Zoetermeer, the Netherlands) in TBS-Tween 20 [TBS-T; 10 mmol/L Tris (pH 8.0), 150 mmol/L NaCl, 0.0025% Tween 20] at room temperature for 1 hour and incubated overnight at 4°C with the kit-provided mouse monoclonal antibody directed against Rac1 (1:500; Chemicon) diluted in 5% bovine serum albumin/TBS-T. After the membrane was washed thrice for 5 minutes with TBS-T, it was incubated with 5% milk/TBS-T, containing horseradish peroxidase–linked antimouse immunoglobulin G secondary antibody, for 1 hour at room temperature. After three TBS-T washing steps of 15 minutes, Rac1 protein was visualized on photography film by enhanced chemoluminescence. Cdc42 protein was visualized on the same blot. Therefore, the Rac1 blot was stripped for 15 minutes in stripping buffer (Pierce, Rockford, IL) and washed thrice with TBS-T. After reassuring that no Rac1 signal was left on the membrane, the blots were blocked again with 10% milk in TBS-T for 1 hour, incubated overnight with the kit-provided mouse monoclonal antibody directed against Cdc42 (1:250; Chemicon), and then incubated with horseradish peroxidase–linked antimouse immunoglobulin G secondary antibody for 1 hour. Proteins were visualized on photography film by enhanced chemoluminescence. The films were scanned and band intensities of active and total protein levels were quantified with TINA quantification software (Raytest, Straubenhardt, Germany) and expressed relative to the band intensities of untreated samples (set at 1.00).

Statistical Analysis

The differences in the effects among the anticancer agents on migration, invasion, organization, and the activities of

Rac1/Cdc42 were statistically analyzed by one-way ANOVA followed by the least significant difference adjustment with SPSS software (SPSS, Inc., Chicago, IL). The level of significance was set at $P < 0.05$.

Results

Determination of HNTCs of Drugs in HUVECs

The antiproliferative effects of cisplatin, doxorubicin, docetaxel, epothilone B, and vinblastine in HUVECs were determined by the MTT assay. Cells were exposed to the drugs for 1 hour, followed by a 96-hour drug-free period. The IC_{50} (mean values) and the HNTC values, as fixed concentrations used in the experiments, are shown in Table 1. Epothilone B was most potent in inhibiting HUVEC proliferation (HNTC, 1 nmol/L), followed by docetaxel (10 nmol/L), vinblastine (10 nmol/L), doxorubicin (100 nmol/L), and cisplatin (10 μmol/L). Mean IC_{50} values were 2- to 15-fold higher than HNTCs and potency followed the same sequence of the drugs. In all further experiments, parallel MTT assays were done to check for drug effects at HNTCs on proliferation because endothelial cells were derived from umbilical veins of different donors. Inhibition of treated cell growth had to be <10% as compared with control cell growth to ensure the use of HNTCs. The last column of Table 1 shows the mean percentage of cell growth when HUVECs were exposed to HNTCs.

Microtubule-Targeting Agents Inhibit HUVEC Migration

Migration of HUVECs was analyzed in the wound assay. A time course of the wound closure up to 12 hours is illustrated by a representative experiment (Fig. 1A). Control cells filled the wound by ~50% after 12 hours. Docetaxel, and to a minor extent epothilone B and vinblastine, slowed down the migration of HUVECs. Figure 1B depicts wound closure at 12 hours after treatment as a percentage of control wound width. HNTCs of cisplatin and doxorubicin did not affect motility of HUVECs; wound closure was 91.8 ± 5.5% and 89.5 ± 5.7% (mean ± SE), respectively. The microtubule-targeting agents significantly inhibited HUVEC migration at HNTCs. Inhibition by docetaxel was most pronounced; at 12 hours, only 44.3 ± 3.9% of the wound was filled as compared with control migration ($P < 0.001$). On exposure to epothilone B and vinblastine, wound closure was 58.9 ± 5.2% ($P < 0.001$) and 69.7 ± 6.3% ($P < 0.001$), respectively. Docetaxel was more effective in the inhibition of migration than epothilone B ($P < 0.05$) and vinblastine ($P < 0.01$).

Microtubule-Targeting Agents Inhibit HUVEC Invasion through Matrigel

HUVEC invasion was investigated in a transwell system, in which cells were allowed to invade through Matrigel in the direction of a chemoattractant (recombinant human vascular endothelial growth factor) for 24 hours. In agreement with the results obtained from the migration assay, docetaxel showed to be most effective in the inhibition of HUVEC invasion as compared with that induced by the other microtubule-targeting agents, although the differences between these agents were not significant (Fig. 2). When the invasion of untreated cells was set at 100%, only 46.0 ± 8.2% (mean ± SE) cell invasion was measured after docetaxel treatment ($P < 0.001$). Epothilone B–treated cells invaded 63.8 ± 7.4% ($P < 0.01$) whereas vinblastine-treated cells invaded 67.3 ± 10.4% ($P < 0.02$). Cisplatin and doxorubicin did not significantly influence HUVEC invasion, as the percentages were 85.7 ± 7.1% and 87.5 ± 5.4%, respectively.

Microtubule-Targeting Agents Inhibit HUVEC Organization

Organization of endothelial cells into precord-like structures on Matrigel can be regarded as an early onset of tube formation. Organization patterns of HUVECs were captured after 24 hours. Untreated cells formed the well-known cord-like structures, which were also visible in samples that were treated with either cisplatin or doxorubicin (Fig. 3A–C). Quantification revealed that the relative number of cell-cell contacts for cisplatin was 110.1 ± 7.6% (mean ± SE), and for doxorubicin this was 104.2 ± 16.6%, which was not significantly different from the number of contacts in control cells (set at 100%; Fig. 3G). Aberrant organization structures were observed after treatment with microtubule-targeting agents; HUVECs showed less contacts with neighboring cells and extensions emerging from single cells did not reach far enough to contact adjacent cells (Fig. 3D–F). Docetaxel (30.0 ± 6.2%), epothilone B (20.7 ± 11.2%), and vinblastine (30.5 ± 10.1%) all significantly prevented the formation of cell-cell contacts as compared with control cells ($P < 0.001$).

Table 1. Antiproliferative effects and HNTCs (fixed) of the different anticancer agents in HUVECs after a 1-hour drug exposure period followed by a 96-hour drug-free period

Drug	IC_{50} (nmol/L ± SD)	HNTC* (nmol/L)	Endothelial cell growth at HNTC† (% ± SD)
Cisplatin	58,500 ± 5,300	10,000	96.9 ± 14.6
Doxorubicin	1,500 ± 1,400	100	94.9 ± 7.5
Docetaxel	21.3 ± 2.1	10	98.4 ± 13.1
Epothilone B	1.9 ± 1.9	1	100.1 ± 6.4
Vinblastine	71.5 ± 4.9	10	84.5 ± 6.0

*Concentration of the drug not yet interfering with proliferation.
†Endothelial cell growth at HNTC expressed as a percentage of control cell growth.

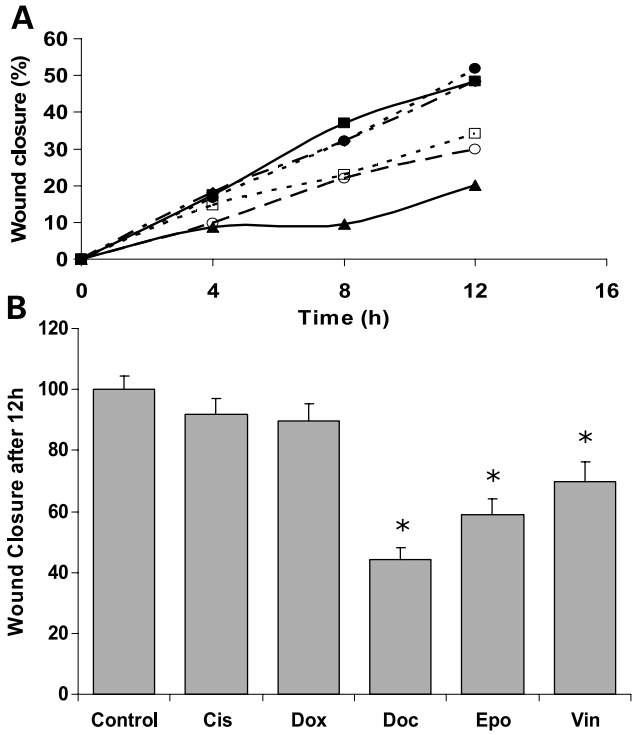

Figure 1. Migration assay. HUVECs were seeded to confluence and incubated with drugs (HNTC) for 1 h. A wound was then applied with a pipette tip and the cells were allowed to migrate for 12 h. **A,** typical experiment showing a time course of a wound refilling with HUVECs: ●, control cells; ■, 10 μmol/L cisplatin; ♦, 100 nmol/L doxorubicin; ▲, 10 nmol/L docetaxel; ○, 1 nmol/L epothilone B; □, 10 nmol/L vinblastine. **B,** wound closure at 12 h of the treated HUVECs as compared with that of control cell migration (set at 100%). *Columns,* mean of at least three separate experiments, each with eight distinct wound thickness measurements; *bars,* SE, *, $P < 0.001$.

Microtubule-Targeting Agents Affect the Integrity of the Cytoskeleton

The structural changes in endothelial cell morphology on inhibition of motility were examined by visualization of two key components of the cytoskeleton, tubulin and F-actin, after a 1-hour drug exposure (HNTCs) and subsequent wounding of the cell monolayer. At 8 hours after wounding, images from the structures of the tubulin and actin cytoskeleton were captured by digital imaging microscopy and the intensity of the tubulin staining signal was measured (Fig. 4). Untreated cells migrated from the monolayer in a left direction into the wound (Fig. 4A). Actin stress fibers were formed in the cell body and cellular actin protrusions in the direction of the wound were filled with tubulin, which indicated correct polarization and an active role for both cytoskeletal components in HUVEC motility. The same patterns were visible in cells treated with cisplatin or doxorubicin (Fig. 4B and C) and the intensity of tubulin staining (mean ± SE) was not significantly different from that of control cells (relative intensity, 1.0 ± 0.03 and 0.99 ± 0.02 as compared with control cells, respectively). It is apparent that these agents do not interfere with tubulin and actin integrity at subtoxic concentrations.

HUVECs treated with microtubule-targeting agents (HNTC) displayed a dissimilar pattern of tubulin and actin than that of control cells. Cells seemed to reside on the edge of the monolayer and showed no clear intention to move into the wound. Both docetaxel (1.2 ± 0.03) and epothilone B (1.17 ± 0.04) treatment led to a significantly higher signal intensity of tubulin staining as compared with that of control cells ($P < 0.01$; Fig. 4D and E), but the visually less intensive staining pattern of vinblastine-treated cells (0.98 ± 0.03) was not significantly different from that of control cells (Fig. 4F). Thus, a short exposure period to very low concentrations of microtubule-targeting agents seems to be sufficient to impede tubulin integrity, which will likely influence the proper functioning of the actin cytoskeleton.

In a separate experiment, the F-actin structure of endothelial cells at the edge of a wound was visualized in more detail (Fig. 5). Control cells (Fig. 5A) displayed actin extensions at the rim of the cell and actin stress fibers throughout the cell body, both in the direction of movement (indicated by the arrow). The overall actin arrangement in cells treated with either cisplatin (Fig. 5B) or doxorubicin (Fig. 5C) was similar to that of control cells. HUVECs treated with the microtubule-targeting agents, however, contained less actin stress fibers. Instead, rings of F-actin formed around the nucleus, suggesting loss of correct cell polarization. Moreover, actin protrusions in the direction of movement were virtually absent at the leading edge of most cells (Fig. 5D–F).

Microtubule-Targeting Agents Inhibit Activity of Rac1 and Cdc42

Because motility of endothelial cells is dependent on the functioning of Rac1 and Cdc42, the activities of these molecules were measured after drug treatment. Activity of

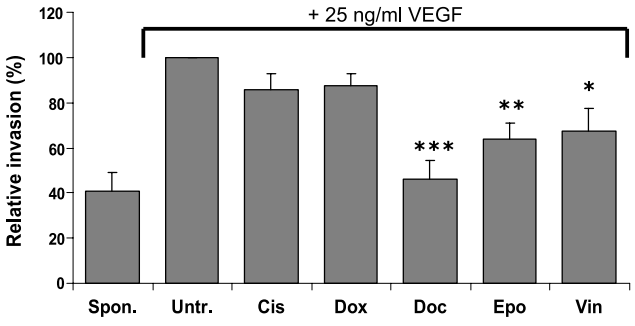

Figure 2. Invasion assay. HUVECs were seeded on top of a Matrigel layer (5 μg) in a transwell insert. Cells were treated with drugs (HNTC) for 1 h (10 μmol/L cisplatin, 100 nmol/L doxorubicin, 10 nmol/L docetaxel, 1 nmol/L epothilone B, 10 nmol/L vinblastine), after which a chemoattractant (25 ng/mL recombinant human vascular endothelial growth factor) was added to the lower compartment of the transwell system. The number of invaded cells was assessed after 24 h by measuring the amount of liberated calcein from calcein-AM (5 μmol/L) that was added to the lower compartment. Invasion towards the applied vascular endothelial growth factor gradient by untreated cells was set at 100%. *Columns,* mean of at least three separate experiments; *bars,* SE. *, $P < 0.02$; **, $P < 0.01$; ***, $P < 0.001$.

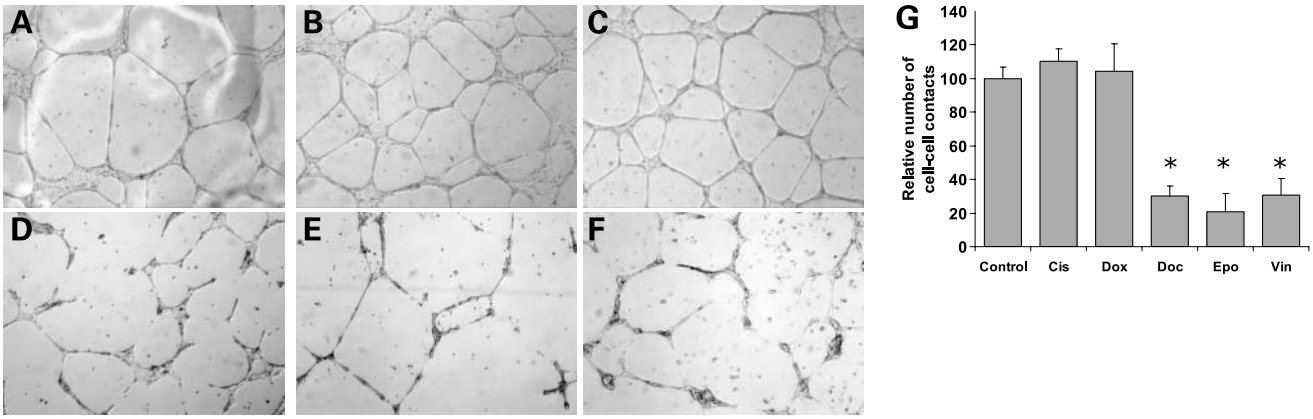

Figure 3. Organization assay. HUVECs were collected in test tubes in which they were exposed to drugs (HNTC) for 1 h. Then, cells were seeded on top of a Matrigel layer. Organization structures were visualized after 24 h by confocal laserscan microscopy. **A,** untreated HUVECs; **B,** HUVECs treated with 10 μmol/L cisplatin; **C,** 100 nmol/L doxorubicin; **D,** 10 nmol/L docetaxel; **E,** 1 nmol/L epothilone B; **F,** 10 nmol/L vinblastine. Representative of three separate experiments (magnification, ×25; bar, 200 μm). **G,** number of cell-cell contacts of treated HUVECs as compared with the number of control cells (set at 100%). *Columns,* mean of at least three experiments; *bars,* SE. *, $P < 0.01$.

both Rac1 and Cdc42 is tightly regulated by actin and tubulin dynamics; disturbances in the microtubule/actin integrity induced by docetaxel, epothilone B, or vinblastine might result in a loss of function of these two key molecules in the onset of cell migration.

After a 1-hour drug exposure, active Rac1 and Cdc42 were pulled down from total cell lysates and compared with total levels of the proteins by Western blot (Fig. 6A and B). Total levels of both Rac1 and Cdc42 remained the same in HUVECs after treatment with each of the drugs. Ratios between active and total protein levels were calculated to analyze drug effects on the activity of Rac1 (Fig. 6C) and Cdc42 (Fig. 6D). Cisplatin (respective ratios of 1.04 ± 0.02 and 1.05 ± 0.37; mean ± SD) and doxorubicin (respective ratios of 0.99 ± 0.11 and 0.97 ± 0.46) had no effect on the activities of these Rho GTPases. Activity of both Rac1 and Cdc42 was potently inhibited by the microtubule-targeting agents. Docetaxel treatment resulted in activity ratios of 0.58 ± 0.04 and 0.53 ± 0.23 for Rac1 and Cdc42, respectively. Epothilone B activity ratios were 0.76 ± 0.17 and 0.51 ± 0.23, whereas vinblastine ratios were 0.63 ± 0.10 and 0.34 ± 0.10, for Rac1 and Cdc42, respectively. When Rac1 ($P < 0.05$) and Cdc42 ($P < 0.02$) activity ratios for all microtubule-targeting agents were grouped and compared with control ratios, a significant difference was calculated.

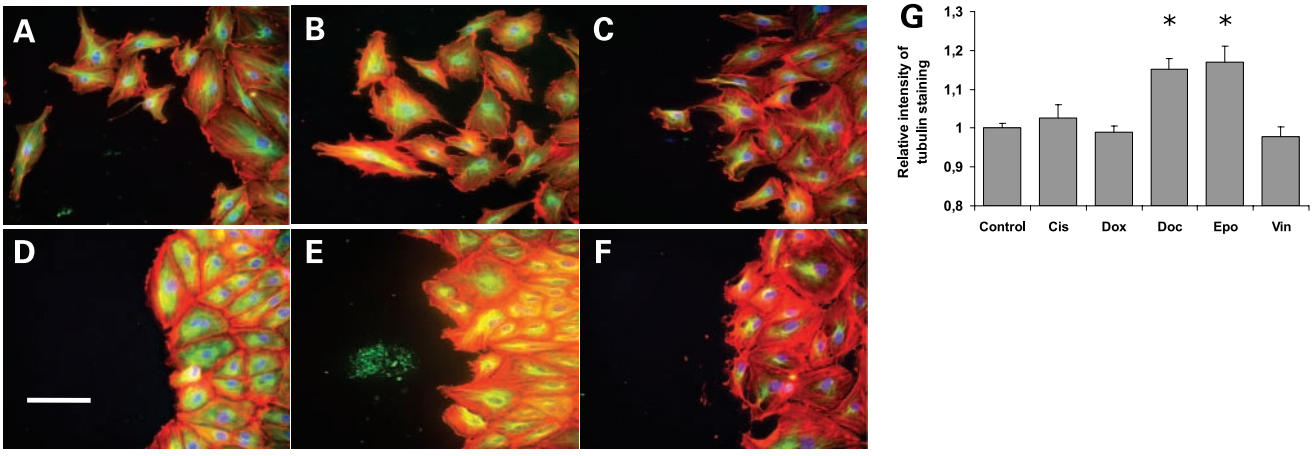

Figure 4. Effects of anticancer agents on the composition of the actin and tubulin cytoskeleton of HUVECs. β-Tubulin (*green*), F-actin (*red*), and nuclear (*blue*) staining of cells after they have grown to confluence, treated with drugs (HNTC) for 1 h, wounded with a Millipore membrane, and allowed to migrate for 8 h. In all images, acquired by live-image fluorescence microscopy, the cell monolayer is on the right and the wound on the left. **A,** untreated HUVECs; **B,** HUVECs treated with 10 μmol/L cisplatin; **C,** 100 nmol/L doxorubicin; **D,** 10 nmol/L docetaxel; **E,** 1 nmol/L epothilone B; **F,** 10 nmol/L vinblastine. Bar, 50 μm. **G,** intensity of tubulin staining of treated HUVECs as a ratio of control cell staining (set at 1.0). *Columns,* mean of at least eight microscopy images collected in four individual experiments; *bars,* SE. *, $P < 0.01$.

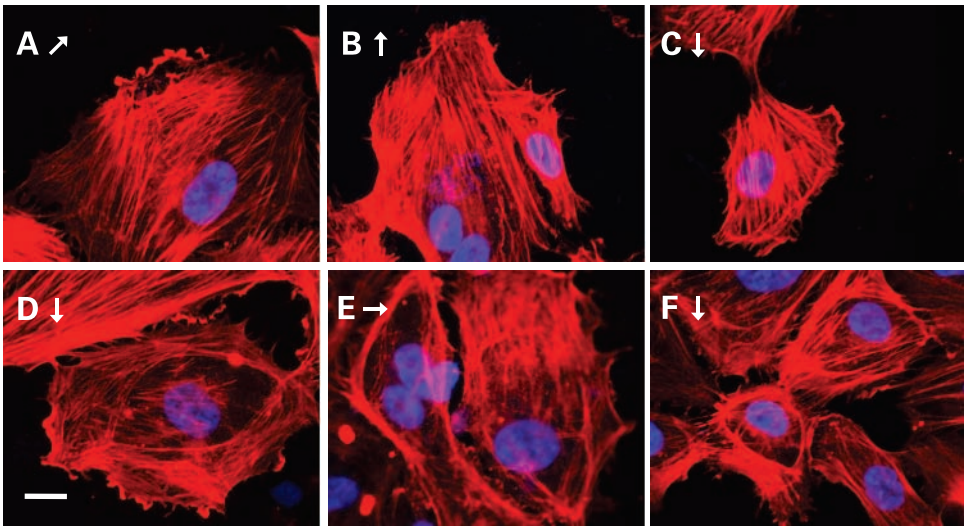

Figure 5. Effects of anticancer agents on the composition of the actin cytoskeleton of HUVECs. F-actin (*red*) and nuclear (*blue*) staining of HUVECs that received the same treatment as described in Fig. 5. Images were acquired by live image fluorescence microscopy. *Arrows,* direction of supposed cell movement. **A**, untreated HUVECs; **B**, HUVECs treated with 10 μmol/L cisplatin; **C**, 100 nmol/L doxorubicin; **D**, 10 nmol/L docetaxel; **E**, 1 nmol/L epothilone B; **F**, 10 nmol/L vinblastine. Bar, 10 μm.

Discussion

We show that subtoxic concentrations of microtubule-targeting agents (docetaxel, epothilone B and vinblastine) potently inhibit *in vitro* angiogenesis features in HUVECs (i.e., endothelial cell migration, endothelial cell invasion, and endothelial cell formation into tubelike structures) whereas subtoxic doses of cisplatin and doxorubicin do not display such effects. Although the net result of equitoxic concentrations on the inhibition of endothelial cell motility was similar for the three classes of microtubule-targeting agents, docetaxel, epothilone B, and vinblastine, slight differences were observed. Docetaxel was most efficient in the inhibition of migration ($P < 0.05$) and invasion, although the latter finding was not significant. Both inhibition of tubulin polymerization by vinblastine and depolymerization by docetaxel and epothilone B impeded cytoskeletal changes required for movement. All three compounds prevented activation of both Rac1 and Cdc42, resulting in disturbance of actin stress fiber formation and the appearance of F-actin rings around the endothelial cell nucleus.

To our knowledge, this is the first study that compares the antiangiogenic properties of different anticancer agents at both subtoxic and equitoxic concentrations. To exclude

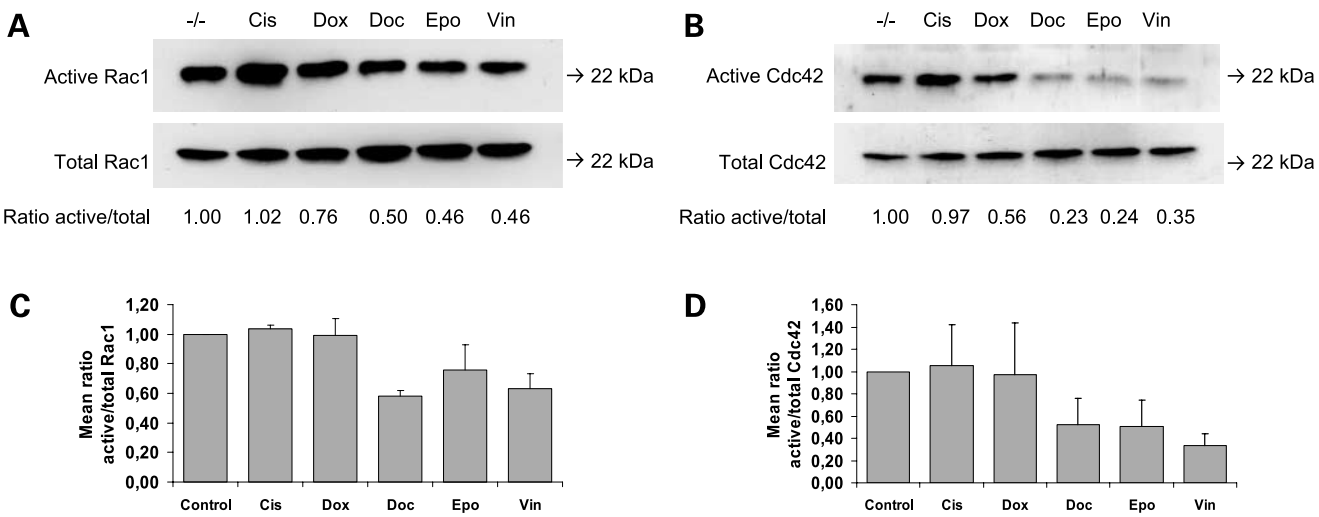

Figure 6. Effects of anticancer agents on the activity of Rac1 and Cdc42 in HUVECs. Semiconfluent cells in minimal medium were stimulated by adding complete culture medium in the presence or absence of the drugs (HNTCs) for 1 h (10 μmol/L cisplatin, 100 nmol/L doxorubicin, 10 nmol/L docetaxel, 1 nmol/L epothilone B, and 10 nmol/L vinblastine). Then, total protein was isolated from the cells and active Rac1/Cdc42 was separated. Both the total protein and active Rac1/Cdc42 samples were subjected to 12% PAGE, followed by Western blot. To acquire comparable signal intensities, the signal for active Rac1/Cdc42 was obtained by capturing the chemiluminescence reaction for 30 min, whereas total Rac1/Cdc42 was obtained after a 15-min exposure. The ratio between the intensity of the active Rac1/Cdc42 signal and the intensity of the total Rac1/Cdc42 signal was calculated. The ratios of untreated cells were set at 1.00. **A** and **B**, bands of active and total Rac1 and Cdc42, respectively, from a representative experiment. **C** and **D**, *columns,* mean active versus total Rac1 (**C**) and Cdc42 (**D**) protein ratios from three separate experiments; *bars,* SE.

an effect on endothelial cell proliferation, each individual experiment was monitored with a parallel MTT assay; the degree of cell growth after treatment had to be ~90% as compared with control cell growth for that experiment to be valid. A set of well-known *in vitro* angiogenesis assays (wound assay, transwell invasion assay, and organization assay) were chosen. HUVECs of different donors were used to exclude observations that can only be attributed to a particular endothelial cell source or immortalized cell line. We expect that the angiogenic behavior of HUVECs reflects that of microvascular endothelial cells derived from tumor tissue. Drug-exposure periods of 1 hour were selected because in patients the anticancer agents analyzed are either given by bolus injections or infusions of 1 to 3 hours. In our experiments, HNTCs of the different anticancer agents were well below the peak plasma concentrations that are generally reached in patients. For cisplatin, a 1-hour infusion of 75 mg/m^2 will lead to a maximum plasma concentration of ~14 μmol/L of intact cisplatin (20). The concentrations are, for doxorubicin, ~1 μmol/L when given as a bolus injection of 60 mg/m^2 (21); for docetaxel, ~4 μmol/L on infusion of 75 to 100 mg/m^2 for 1 hour (22); and for vinblastine, ~160 nmol/L when given as a bolus injection of 7 to 10.8 mg/m^2 (23). Peak plasma levels of epothilone B in humans have yet to be reported.

Cisplatin does not inhibit *in vitro* angiogenesis at a subtoxic concentration in our experiments. These observations are in agreement with other studies in which nontoxic concentrations of cisplatin did not interfere with angiogenic features (24–26). For doxorubicin, we also showed that 1-hour incubations with a subtoxic concentration did not have any antiangiogenic effects. This is also in concert with earlier findings that showed that only toxic concentrations of doxorubicin are able to inhibit angiogenic properties (9, 25). We conclude that compounds affecting DNA integrity do not directly interfere with cell motility.

Members of three classes of microtubule-targeting agents used in this study were able to inhibit angiogenic features of HUVECs at HNTCs. The taxane family of anticancer agents has been reported to possess antiangiogenic potential. When compared with paclitaxel, docetaxel inhibits angiogenesis more potently (4, 6, 27), but drug concentrations used in the experiments often inhibited endothelial cell proliferation as well. Hotchkiss et al. (5) have been the first to highlight the potential of nontoxic docetaxel concentrations in angiogenesis inhibition. The epothilones are a relatively new class of anticancer agents and evidence for antiangiogenic properties is limited. Epothilone B has been described to have superior potency to paclitaxel in inhibition of endothelial cell proliferation *in vitro* after continuous low-dose administration (9). Woltering et al. (8) have reported that epothilone B inhibits *in vitro* angiogenesis at relatively high concentrations. Both observations do not provide insight in angiogenesis inhibition at subtoxic concentrations. Little is known about the potency of the different family members of the Vinca alkaloids in inhibiting angiogenesis. It has been reported that vincristine, vinorelbine, and vinflunine are all able to shut down tumor vasculature in *in vivo* models (28). The antiangiogenic effects of low vinblastine concentrations are well established in a variety of *in vitro* and *in vivo* experiments (10, 11). Our data underline the ability of microtubule-targeting agents to inhibit *in vitro* angiogenesis at subtoxic concentrations of which docetaxel seemed to be slightly more efficient in inhibiting endothelial cell motility than epothilone B and vinblastine. Furthermore, we established the antiangiogenic potential of subtoxic concentrations of epothilone B.

Microtubules are essential in the orchestration of endothelial cell motility (16). It is likely that the specific mechanism of action of docetaxel, epothilone B, and vinblastine (i.e., interference with microtubule dynamics) is responsible for inhibition of the angiogenic process. Indeed, in our endothelial cells treated with docetaxel or epothilone B (Fig. 4D and E), the β-tubulin staining was significantly more intense as compared with control cells, indicating stabilization of the microtubules already after treatment with low concentrations. Hotchkiss et al. (5) have reported that docetaxel did not visibly interfere with microtubule morphology at nontoxic (1 nmol/L, 24-hour incubation), yet angiogenesis-inhibiting concentrations. When in that same experiment 10 nmol/L docetaxel was applied for 24 hours, changes in microtubule structures were visible, but endothelial cell proliferation was also affected. We observed that at 1-hour exposure, 10 nmol/L docetaxel did not yet inhibit cell growth, but rapidly altered microtubule morphology. The vinblastine-treated cells (Fig. 4F) showed less intense tubulin staining images, but quantification was not different from control cell fluorescence intensity. Still, a 1-hour exposure to the nontoxic concentration of 10 nmol/L already resulted in inhibition of polymerization.

Microtubules and actin are known to cooperate to modify cell shape and establish cell polarity either directly or by regulation of signaling molecules, such as the Rho GTPases (29). Actin stress fibers are visible in migrating cells at the edge of a wound as visualized in our control cells (Fig. 5A). These fibers were absent in cells at the leading edge after treatment with the microtubule-targeting agents (Fig. 5D–F). Instead of stress fiber formation, we observed a ring of F-actin around the nucleus in a subset of cells. Nuclear actin ring formation has been observed in MCF-7 cells treated with either paclitaxel or docetaxel (30). In addition, Pletjushkina et al. (31) have reported the development of circumferential actin bundles instead of straight bundles in rat fibroblasts after treatment with paclitaxel. Thus, stabilization of microtubules or inhibition of microtubule depolymerization results in changes in actin organization. Because microtubule polymerization is required for actin polymerization (29), a process inhibited by vinblastine, this is manifested by disorganized F-actin as well (Fig. 5F).

Disturbances in actin structures may be the consequence of inhibition of Rho GTPases action. Docetaxel and epothilone B prevented Rac1 activation (Fig. 6A), which might clarify the absence of actin stress fibers in endothelial

cells after treatment. Rac1 is activated in lamellipodia on microtubule polymerization and stimulates actin stress fiber assembly. Actin polymerization, in turn, leads to retrograde actin flow and rupture of buckled actin-associated microtubules and subsequent microtubule polymerization (32). Based on our findings, we propose that interference in this positive feedback loop through inhibition of microtubule dynamics will result in a decrease of Rac1 activity and subsequent inhibition of actin stress fiber formation. Although Rac1 is activated on microtubule polymerization (32), our results show that stabilization of microtubules or inhibition of polymerization prevents activation of Rac1. This is most probably due to reduced microtubule dynamics, as is the consequence from taxane treatment (33). In our experiments, Rac1 activity was already inhibited 1 hour after treatment, implicating an essential role for microtubule dynamics in the onset of migration. The fact that microtubule-targeting agents inhibit Rac1 activity in HUVECs is in line with the observation of Hu et al. (34) that paclitaxel decreased the shear stress-induced Rac1 activation and concomitant migration speed of bovine aortic endothelial cells. In addition, paclitaxel can prevent the formation of Rac1-GTP levels, as shown in fibroblasts stimulated to initiate microtubule polymerization (35). The same group of Waterman-Storer et al. (35) has also shown that an inhibitor of microtubule polymerization, nocodazole, reduced Rac1-GTP to levels of control fibroblasts, whereas washout of drug rapidly resulted in increasing Rac1-GTP amounts. In line with these data, we showed that inhibition of polymerization by vinblastine also reduced active Rac1.

We hypothesized that the decreased endothelial cell motility, lack of contractile actin bundles, and, in particular, the formation of F-actin rings around the nucleus in cells treated with microtubule-targeting agents would be associated with disturbed polarization of the cells and blocked activity of Cdc42 (Fig. 6B). If not inhibited, Cdc42 mediates correct polarization of cells to migrate in the proper direction (36). Moreover, Cdc42 regulates the precise orientation of the centrosome in migrating cells (14, 37). Hotchkiss et al. (5) have shown that docetaxel impairs repositioning of the centrosome in migrating cells, hence supporting our finding that docetaxel inhibits Cdc42 activity. It is also known that microtubule dynamics are essential for activity of Rho guanine nucleotide exchange factors, which in turn activate the Rho GTPases (38). It is likely that inhibition of microtubule dynamics interferes with Rho guanine nucleotide exchange factor activity and Rho GTPase function, which already occur within 1 hour after treatment. The exact mechanism of Cdc42 inhibition on treatment with microtubule-targeting agents should be further explored as well as the possible involvement of other family members of the Rho GTPases.

In conclusion, interference with microtubule dynamics by treatment of endothelial cells with microtubule-targeting agents prevents activation of Rac1 and Cdc42. This is associated with a negative effect on correct polarization, the formation of lamellipodia, actin polymerization, and subsequent stress fiber formation. As a consequence, the cells are not able to pinpoint the direction of movement whereas motility itself is physically hampered by disordered microtubule and actin cytoskeleton structures. Furthermore, communication between endothelial cells is disturbed, because of which precapillary organization is obstructed. The overall effect of the antiangiogenic properties of subtoxic concentrations of microtubule-targeting agents will result in reduced vessel formation *in vivo*. Therefore, these compounds may provide opportunities for inhibition of angiogenesis not only in malignancies but also in diseases associated with an abnormal neovascularization process.

Acknowledgments

We thank Ing. Henk Dekker for expert technical assistance with the confocal laserscan microscope.

References

1. Jordan MA, Wilson L. Microtubules as a target for anticancer drugs. Nat Rev Cancer 2004;4:253–65.

2. Schimming R, Hunter NR, Mason KA, Milas L. Inhibition of tumor neoangiogenesis and induction of apoptosis as properties of docetaxel (Taxotere). Mund Kiefer Gesichtschir 1999;3:210–2.

3. Sweeney CJ, Miller KD, Sissons SE, et al. The antiangiogenic property of docetaxel is synergistic with a recombinant humanized monoclonal antibody against vascular endothelial growth factor or 2-methoxyestradiol but antagonized by endothelial growth factors. Cancer Res 2001;61:3369–72.

4. Vacca A, Ribatti D, Iurlaro M, et al. Docetaxel versus paclitaxel for antiangiogenesis. J Hematother Stem Cell Res 2002;11:103–18.

5. Hotchkiss KA, Ashton AW, Mahmood R, et al. Inhibition of endothelial cell function *in vitro* and angiogenesis *in vivo* by docetaxel (Taxotere): association with impaired repositioning of the microtubule organizing center. Mol Cancer Ther 2002;1:1191–200.

6. Grant DS, Williams TL, Zahaczewsky M, Dicker AP. Comparison of antiangiogenic activities using paclitaxel (Taxol) and docetaxel (Taxotere). Int J Cancer 2003;104:121–9.

7. Goodin S, Kane MP, Rubin EH. Epothilones: mechanism of action and biologic activity. J Clin Oncol 2004;22:2015–25.

8. Woltering EA, Lewis JM, Maxwell PJ, et al. Development of a novel *in vitro* human tissue-based angiogenesis assay to evaluate the effect of antiangiogenic drugs. Ann Surg 2003;237:790–8.

9. Bocci G, Nicolaou KC, Kerbel RS. Protracted low-dose effects on human endothelial cell proliferation and survival *in vitro* reveal a selective antiangiogenic window for various chemotherapeutic drugs. Cancer Res 2002;62:6938–43.

10. Vacca A, Iurlaro M, Ribatti D, et al. Antiangiogenesis is produced by nontoxic doses of vinblastine. Blood 1999;94:4143–55.

11. Klement G, Baruchel S, Rak J, et al. Continuous low-dose therapy with vinblastine and VEGF receptor-2 antibody induces sustained tumor regression without overt toxicity. J Clin Invest 2000;105:R15–24.

12. Soga N, Namba N, McAllister S, et al. Rho family GTPases regulate VEGF-stimulated endothelial cell motility. Exp Cell Res 2001;269:73–87.

13. Nieuw Amerongen GP, Koolwijk P, Versteilen A, van Hinsbergh VW. Involvement of RhoA/Rho kinase signaling in VEGF-induced endothelial cell migration and angiogenesis *in vitro*. Arterioscler Thromb Vasc Biol 2003;23:211–17.

14. Etienne-Manneville S, Hall A. Cdc42 regulates GSK-3β and adenomatous polyposis coli to control cell polarity. Nature 2003;421:753–6.

15. Etienne-Manneville S, Hall A. Integrin-mediated activation of Cdc42 controls cell polarity in migrating astrocytes through PKCζ. Cell 2001;106:489–98.

16. Ridley AJ. Rho GTPases and cell migration. J Cell Sci 2001;114:2713–22.

17. Raftopoulou M, Hall A. Cell migration: Rho GTPases lead the way. Dev Biol 2004;265:23–32.

18. Waterman-Storer CM, Salmon E. Positive feedback interactions between microtubule and actin dynamics during cell motility. Curr Opin Cell Biol 1999;11:61 – 7.

19. van Hinsbergh VW, Draijer R. Culture and characterization of human endothelial cells. In: Oxford: University Press Shaw A J; 1996. p. 87 – 110.

20. Verschraagen M, Boven E, Ruijter R, et al. Pharmacokinetics and preliminary clinical data of the novel chemoprotectant BNP7787 and cisplatin and their metabolites. Clin Pharmacol Ther 2003;74:157 – 69.

21. Brenner DE, Grosh WW, Noone R, et al. Human plasma pharmacokinetics of doxorubicin: comparison of bolus and infusional administration. Cancer Treatment Symposia 1984;3:77 – 83.

22. Bruno R, Hille D, Riva A, et al. Population pharmacokinetics/pharmacodynamics of docetaxel in phase II studies in patients with cancer. J Clin Oncol 1998;16:187 – 96.

23. Nelson RL, Dyke RW, Root MA. Comparative pharmacokinetics of vindesine, vincristine and vinblastine in patients with cancer. Cancer Treat Rev 1980;7 Suppl 1:17 – 24.

24. Li D, Williams JI, Pietras RJ. Squalamine and cisplatin block angiogenesis and growth of human ovarian cancer cells with or without HER-2 gene overexpression. Oncogene 2002;21:2805 – 14.

25. Hayot C, Farinelle S, De Decker R, et al. *In vitro* pharmacological characterizations of the anti-angiogenic and anti-tumor cell migration properties mediated by microtubule-affecting drugs, with special emphasis on the organization of the actin cytoskeleton. Int J Oncol 2002;21:417 – 25.

26. Kumar P, Benedict R, Urzua F, et al. Combination treatment significantly enhances the efficacy of antitumor therapy by preferentially targeting angiogenesis. Lab Invest 2005;85:756 – 67.

27. Ng SS, Figg WD, Sparreboom A. Taxane-mediated antiangiogenesis *in vitro*: influence of formulation vehicles and binding proteins. Cancer Res 2004;64:821 – 4.

28. Holwell SE, Hill BT, Bibby MC. Anti-vascular effects of vinflunine in the MAC 15A transplantable adenocarcinoma model. Br J Cancer 2001;84:290 – 5.

29. Etienne-Manneville S. Actin and microtubules in cell motility: which one is in control? Traffic 2004;5:470 – 7.

30. Rosenblum M.D., Shivers RR. ''Rings'' of F-actin form around the nucleus in cultured human MCF7 adenocarcinoma cells upon exposure to both Taxol and Taxotere. Comp Biochem Physiol C Toxicol Pharmacol 2000;125:121 – 31.

31. Pletjushkina OJ, Ivanova OJ, Kaverina IN, Vasiliev JM. Taxol-treated fibroblasts acquire an epithelioid shape and a circular pattern of actin bundles. Exp Cell Res 1994;212:201 – 8.

32. Wittmann T, Waterman-Storer CM. Cell motility: can Rho GTPases and microtubules point the way? J Cell Sci 2001;114:3795 – 803.

33. Goncalves A, Braguer D, Kamath K, et al. Resistance to Taxol in lung cancer cells associated with increased microtubule dynamics. Proc Natl Acad Sci U S A 2001;98:11737 – 42.

34. Hu YL, Li S, Miao H, et al. Roles of microtubule dynamics and small GTPase Rac in endothelial cell migration and lamellipodium formation under flow. J Vasc Res 2002;39:465 – 76.

35. Waterman-Storer CM, Worthylake RA, Liu BP, et al. Microtubule growth activates Rac1 to promote lamellipodial protrusion in fibroblasts. Nat Cell Biol 1999;1:45 – 50.

36. Etienne-Manneville S, Hall A. Rho GTPases in cell biology. Nature 2002;420:629 – 35.

37. Palazzo AF, Joseph HL, Chen YJ, et al. Cdc42, dynein, and dynactin regulate MTOC reorientation independent of Rho-regulated microtubule stabilization. Curr Biol 2001;11:1536 – 41.

38. Krendel M, Zenke FT, Bokoch GM. Nucleotide exchange factor GEF-H1 mediates cross-talk between microtubules and the actin cytoskeleton. Nat Cell Biol 2002;4:294 – 301.

Molecular Cancer Therapeutics

Microtubule-targeting agents inhibit angiogenesis at subtoxic concentrations, a process associated with inhibition of Rac1 and Cdc42 activity and changes in the endothelial cytoskeleton

Marcel N.A. Bijman, Geerten P. van Nieuw Amerongen, Nancy Laurens, et al.

Mol Cancer Ther 2006;5:2348-2357.